Change in the Branch Period of the Step Pattern Formed by a Moving Linear Source —Initial Coarsening and Effect of an Abrupt Change in the Velocity—

Shinji Kondo[a], Masashi Kawaguchi[a], Masahide Sato[b], Makio Uwaha[a]

[a] *Department of Physics, Nagoya University, Furo-cho, Chikusa-ku, Nagoya 464-8602, Japan*
[b] *Information Media Center, Kanazawa University, Kakuma-machi, Kanazawa 920-1192, Japan*

Abstract

We study pattern formation of a step induced by a moving linear source of adatoms, which is related to a step pattern during Ga deposition on Si(111), and possively to a graphene film grown on SiC. Diffusion of adatoms released from the source in front of the step causes wandering instability of the step. Many small intrusions with branches appear, and the characteristic length of the pattern increases untill it reaches a steady state. Coarsening process of the branch period is examined. In the first stage the period increases as $\lambda \sim t^{\nu_1}$, with $\nu_1 \approx 1/4$, increasing slowly with decreasing the velocity of the source. Competition between the intrusions results in a faster growth of the branch period with exponent $\nu_2 \approx 1/2$. Change in the step pattern by an abrupt change in the source velocity is also studied. Branches adjust their period by terminating growth of some branches or increasing their number by tip-splitting. The latter is suppressed by a large stiffness and a metastable state with side branches is seen.

Keywords: A1: Computer simulation, A1: morphological instability, A1: Surface processes, A3: Physical vapor deposition processes, B2: Semiconducting silicon

1. Introduction

A strange comblike pattern of a growing step was observed during Ga deposition onto a Si(111) vicinal face [1]. With Ga deposition, a structural phase transformation of the surface from the $\sqrt{3}\times\sqrt{3}$ structure to the 6.3×6.3 structure is induced near the lower side of a step, and simultaneously Si atoms are released onto the surface. Therefore the moving phase boundary with Ga incorporation acts as a source of Si adsorbed atoms (adatoms) and the step growth occurs with such excess Si atoms. We have modeled this system as a growing step guided by a linear source of adatoms, and suceeded to reproduce the comblike step pattarn in the Monte Carlo simulation [2, 3]. Such a growth guided by an atom source may be found in other systems. Actually, a similar pattern has been reported during epitaxial growth of a graphene sheet from a heated SiC crystal. Si atoms are evaporated from the SiC surface by heating, and a buffer layer of carbon-rich $6\sqrt{3}\times6\sqrt{3}$ structure is first formed. Further evaporation of Si produces a new buffer layer, and the existing buffer layer transforms into graphene. Fingerlike graphene was observed in the lower side near the step, which is probably the source of C atoms [4, 5, 6]. The number of C atoms in graphene is about three times that in a SiC bilayer. Therefore a single or a double bilayer step cannot supply sufficient C atoms to form a graphene layer, as the phase boundary in the Ga/Si sytem. Insufficient supply of C atoms causes wandering instability of the graphene growth front in the diffusion field, and the front forms the comblike pattern [6]. Thus, diffusional growth guided by a linear atom source may be realized under various conditions, and common pattern formation should be observed.

In our previous study [3], we have performed Monte Carlo simulations with a square lattice model. In the model, a step is advancing by incorporating adatoms that are released from a linear source moving in front of the step. The initially straight step is unstable and many intrusions appear at the beginning. Relaxation of the small intrusions and competition between the intrusions result in coarsening of the pattern, and the step soon reaches a steadily growing state where branching period shows a steady profile. The intrusions tend to grow into the $\langle 11\rangle$ directions of the suquare lattice, and the comblike pattern is seen in growth towards the [11] direction. These patterns are markedly different from that of deposition growth [7, 8, 9] or from growth without evaporation [10, 11, 12]. Period λ of branches in the steady state, λ^*, is proportional to $\sqrt{\tilde{\beta}/V_{\rm p}}$, where $\tilde{\beta}$ is the step stiffness and $V_{\rm p}$ the velocity of the moving source.

In the present paper we study coarsening behavior in the initial stage of growth and the change in period by an abrupt change in the source velocity. In **2** we define our model of a step with a linear source of adatoms, and the results of our previous study are summarized in **3**. Initial stage of the wandering instability is studied in **4** with emphasis on coarsening of the wandering pattern. In **5** we study how the period is adjusted when the velocity is changed abruptly. Finally, we summarize our results and discuss about remaining questions in **6**.

Email address: uwaha@nagoya-u.jp ()
URL: http://www.slab.phys.nagoya-u.ac.jp/uwaha/ ()

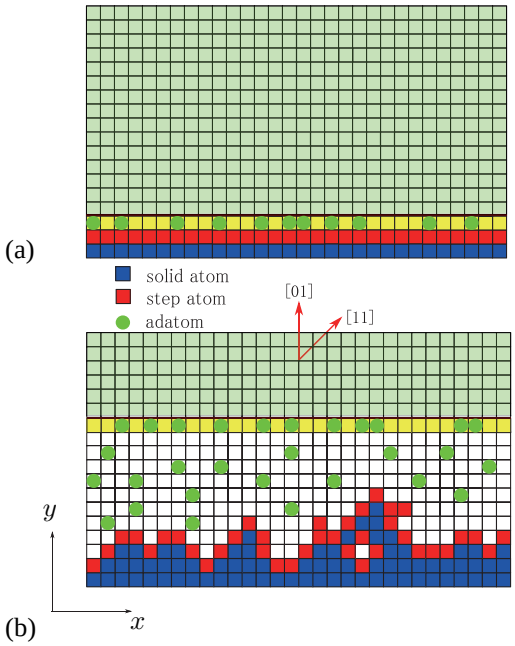

Figure 1: The lattice model for a (01) step. The blue and red squares are solid and step atoms. The green circles are adatoms. The yellow line is the phase boundary, and the green area is the outside. (a) The initial and (b) a later configuration.

2. Model

The model we use was introduced in Ref. [3] to explain the comblike pattern found in Si(001) surface with Ga deposition. The rules for growth of a step and diffusion of adatoms are the same as those of Ref. [8]. Adatoms diffuse on a flat square lattice, which is bound by a step on one side and by a straight phase boundary releasing adatoms and moving at a constant velocity V_p (the location is $y(x,t) = V_\mathrm{p}t$), on the other side. In Fig. 1, we show a magnified view of a (01) step. The lattice is rotated 45° for a (11) step. A periodic boundary condition is imposed in the x direction: the site (x, y) is equivalent to $(x + L, y)$. When an adatom comes next to the step, it may solidify with the probability

$$p_+ = \frac{1}{1 + e^{(\Delta E - \phi)/k_\mathrm{B}T}}, \tag{1}$$

where ΔE is the change in step energy (the kink energy ϵ or half the lateral bond energy times the perimeter length in the unit of the lattice constant) associated with the solidification, and ϕ is the energy gain in solidification. The solidified atom becomes a step atom, and step atoms form an edge of the solid atomic layer. A step atom may "melt" to become an adatom with the probability

$$p_- = \frac{1}{1 + e^{(\Delta E + \phi)/k_\mathrm{B}T}}, \tag{2}$$

where ΔE is the change in step energy associated with the melting. Time increases in each diffusion trail, and the unit of time is so chosen that the diffusion coefficient D_s is unity.

At the start, the step is straight and located near the bottom of the system, and the source is in contact with the step. The

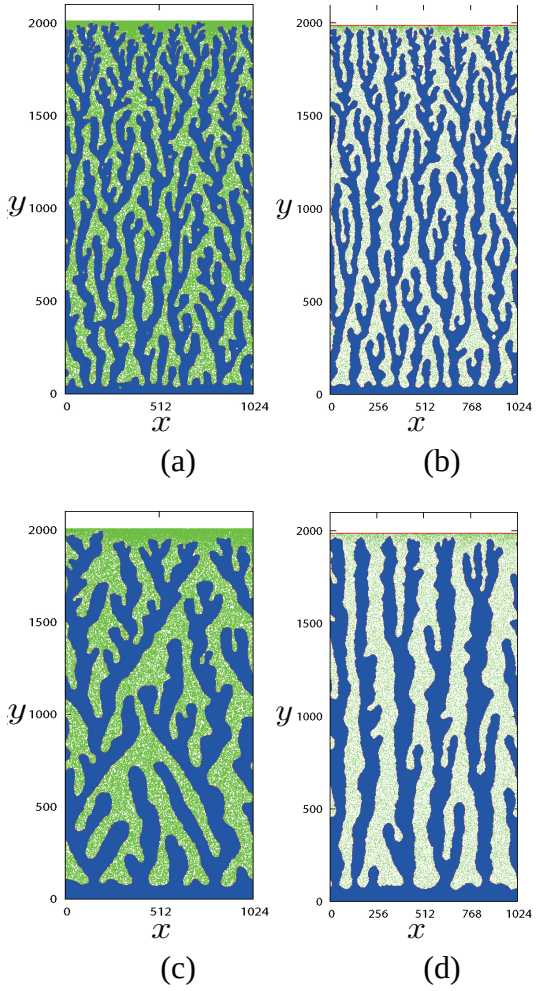

Figure 2: Step patterns induced by the moving linear source of atoms at velocity $V_\mathrm{p} = 0.02$, (a) in the [01] direction and (b) in the [11] direction, and $V_\mathrm{p} = 0.005$, (c) in the [01] direction and (d) in the [11] direction. Blue (dark grey) represents solid layer, and green (light grey) dots represent adatoms.

y direction is either [01] or [11] direction of a square lattice. The motion of the adatom source is realized in the simulation as follows. The linear source initially contains c_0 randomly distributed adatoms per site, and it is the upper boundary of the system. Every time interval V_p^{-1}, a new line of lattice sites with c_0 adatoms per site is added at the top of the system. We use the parameter value $\phi/k_\mathrm{B}T = 3.0$, which gives the equilibrium adatom density as $c_\mathrm{eq}^0 = e^{-\phi/k_\mathrm{B}T} = 0.05$. The adatom density c_0 is chosen to be 0.525. Then, in the long run, half of the system is covered by solid, and the rest is the terrace with the equilibrium number of adatoms. The kink energy is set as $\epsilon/k_\mathrm{B}T = 2.0$ giving stiffness $\tilde{\beta}_{[01]} = 2.76$ and $\tilde{\beta}_{[11]} = 1.23$ [8]. The width of the system is $L = 1024$ (we set the lattice constant as the length unit).

3. Formation of a forest

Typical step patterns formed in the simulation are shown in Fig. 2. These patterns and similar patterns found in a related

model are analyzed in Refs. [2] and [3]. The results are summarized as follows.

1. Wandering instability of the step is induced by the moving linear source of adatoms, and a forestlike pattern of intrusions appears.
2. Because of the anisotropy in the step stiffness, intrusions tend to grow into the ⟨11⟩ directions of the smallest stiffness. As a result, the step growing into the [01] direction produces many branches (Figs. 2(a) and (c)) while the step growing into the [11] direction produces few branches (Figs. 2(b) and (d)). The latter patterns resemble the comblike step pattern found on a Ga deposited Si(111) surface [1] and the finger pattern of a graphene sheet [4, 5, 6].
3. Except for coarsening and local relaxation in the early stage, the global pattern of the step seems steady. In particular period λ of branches, measured by counting number of branches at a certain height, takes a steady value determined by velocity V_p of the source and the kink energy ϵ. Period λ was found to be several times larger than the linearly most unstable wavelength, λ_max, of the wandering instability

$$\lambda_\mathrm{max} = 2\pi\sqrt{\frac{3\Gamma l_\mathrm{D}}{1-c_\mathrm{eq}^0}}, \tag{3}$$

   where $l_\mathrm{D} = D_\mathrm{s}/V_\mathrm{p}$ is a diffusion length corresponding to the source velocity, and $\Gamma = c_\mathrm{eq}^0\tilde{\beta}_{[01]}/k_\mathrm{B}T$ the capillary length for the [01] step (this holds true even for the growth into the [11] direction). Thus the period is determined by the stiffness of the [01] step and the source velocity: $\lambda \sim \sqrt{\tilde{\beta}_{[01]}/V_\mathrm{p}}$. The moving source at a different velocity V_p brings about a similar pattern of the different length scale: the pattern adjusts its characteristic length to follow the guiding source.
4. If V_p is too fast, however, the step cannot follow the source and a fractallike growth at a constant velocity occurs.

In the following, we first study the change in branch period λ during growth, *i.e.* coarsening of the step pattern in the early stage. We also study the adjustment of period λ to an abrupt change in velocity V_p of the source.

4. Coarsening of the step pattern

Period of branches. From the simulation data we deduced the period of branches by two different ways.

In the previous paper [3] we counted the number of branches cut at various height y, and derived period λ^* near the top in the steady state. Here we are interested in early stage of the growth before the steady stage, and we simply count the number at the half-way line to the effective front y_s of the solid layer defined later in Eq. (4). [1] The results are shown in Fig. 3. The coarsening process is divided into two stages, and both stages show

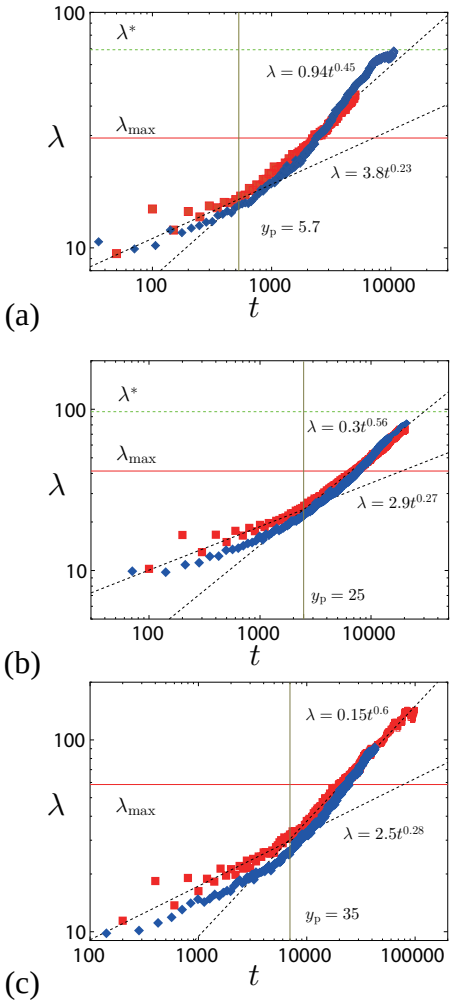

Figure 3: Change of the branch period, λ, as time in the [01] growth (square) and in the [11] growth (diamond). The velocity of the source is (a) $V_\mathrm{p} = 0.02$, (b) $V_\mathrm{p} = 0.01$, (c) $V_\mathrm{p} = 0.005$. Dotted lines are power-law fits, horizontal lines are λ_max, and dotted horizontal lines are the steady state values, λ^*, in Ref. [3], all for the [01] growth.

power-law growth with time. For the [01] growth, the exponent in the first stage is about 1/4 (0.23-0.28) and that in the second stage is about 1/2 (0.45-0.6). The growth in the [11] direction shows a similar behavior. The differences are λ in the first stage is about ten percent smaller, and the exponents in the second stage is slightly larger.

We have also performed Fourier analysis of the step position, $y(x,t)$, as shown in Fig. 4. It is more accurate in the early stage than counting the number of branches, but looses accuracy once the step developes overhangs[2]. The exponents found in the first stage are about the same as those obtained in Fig. 3, but the transition to the second stage is seen much later (about four times). For small source velocities, the exponent increases up to 0.4. The value of the second stage is not reliable because of overhangs.

[1] Since the values of V_p studied in this paper are rather small, we may neglect the effect of relaxation after growth and resultant decrease in the branch number.

[2] We have made Fourier analysis of the highest step position at each x.

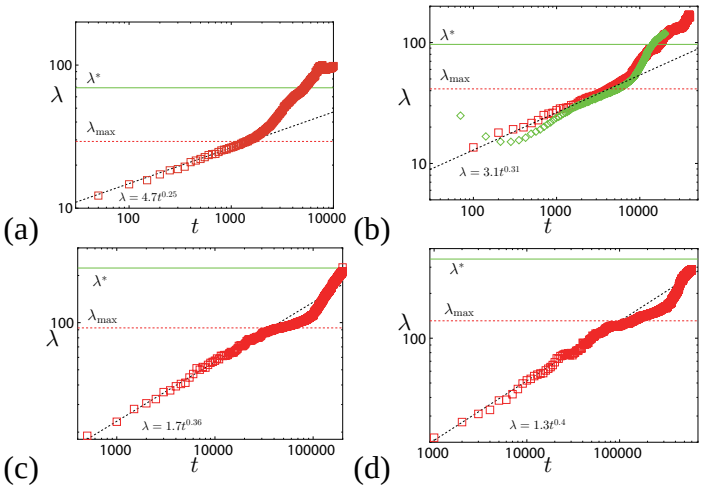

Figure 4: Change of the branch period λ found in the Fourier analysis, with the source velocity (a) $V_p = 0.02$. (b) $V_p = 0.01$. (c) $V_p = 0.002$. (d) $V_p = 0.001$ for the [01] growth (square). In (b), data for the [11] growth are also shown by diamonds. Dotted lines are power-law fits, horizontal lines are $\lambda_{\max}$, and dotted horizontal lines are the steady state values, λ^*, in Ref. [3], for the [01] growth.

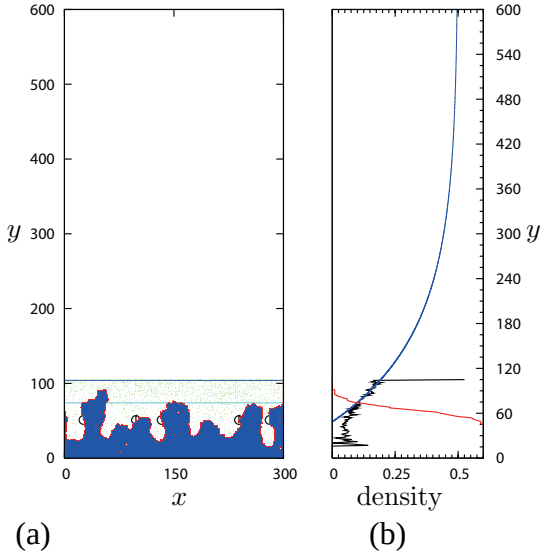

Figure 5: (a) Part of a growth pattern with $V_p = 0.01$ at $t = 10000$ ($y_p = 100$). Circles indicate the position of steps cut at $y_s/2$. (b) Density of solid (red or grey line) and adatoms (black line), and the best fit to the adatom density Eq. (8) (blue or dark grey line).

Diffusion length. The coarsening of the pattern may be related to the change in the diffusion length. To find the diffusion length for each simulation we made an analysis based on the following picture. If we measure density of the solid and that of adatoms averaged over x as a function of the height, y, the profiles at time t, $c_s(y,t)$ and $c(y,t)$, can be interpreted as follows. Most of the solid forest region will show the constant density, $c_s(y) \approx$ const $\equiv c_s = 1/2$, near to an effective sharp front of the growing solid layer (or an averaged position of the growing part of step), defined by

$$c_s y_s(t) = \int_0^{V_p t} c_s(y,t)dy, \tag{4}$$

where $c_s(y,t) = \sum_{x=1}^{L} c_s(x,y,t)/L$. If we regard the system as one-dimensional, the boundary condition for the adatom density, $c(y,t) = \sum_{x=1}^{L} c(x,y,t)/L$, at the solid front, $y = y_s(t)$, is

$$c_s \dot{y}_s(t) = D_s \left.\frac{\partial c}{\partial y}\right|_{y_s(t)}, \tag{5}$$

and at the source, $y = y_p$, is

$$c_0 V_p = c(y_p)V_p + D_s \left.\frac{\partial c}{\partial y}\right|_{y_p = V_p t}. \tag{6}$$

Supposing that a steady state is approximately realized at each moment, the steady state solution of the diffusion equation in the frame of reference moving at velocity $V = \dot{y}_s = V_p$ for the boundary conditions, Eq. (5) and that $c(y \to \infty) = c_0$, is (the latter is necessary for the existence of the steady state in one-dimension)

$$c(y) = \left(c_0 - c_{eq}^0\right)\left[1 - \exp\left(-\frac{V_p}{D_s}(y - y_s)\right)\right] + c_{eq}^0. \tag{7}$$

Substituting Eq. (7) to Eq. (6), it is easily seen that this solution satisfies Eq. (6) automatically. It means that the average density is approximately represented by Eq. (7), and the distance between the step position and the source, $y_p - y_s$, is not uniquely determined. The diffusion length defined from the density gradient is given by $l_D = D_s/V_p$.

Density profile in the simulation. In the above picture we have assumed a steady state, but in reality the density profile must change since the source is initially in contact with the step and the distance $y_p - y_s$ increases with time until the steady state is realized. To analyze the change we measured the density profile $c(y,t)$ and fit it with the function

$$c(y) = \left(c_0 - c_{eq}^0\right)\left[1 - \exp\left(-\frac{y - \tilde{y}_s}{\tilde{l}_D}\right)\right] + c_{eq}^0, \tag{8}$$

where we treat $\tilde{y}_s$ and $\tilde{l}_D$ as fitting parameters.

An example is shown in Fig. 5. The black line in Fig. 5(b) is the adatom density $c(y,t)$ and the red line is the solid density $c_s(y,t)$. The blue line is the best fit Eq. (8) to the upper part of the black line. We checked consistency of the parameters thus found by calculating the mass conservation at y_p. The measured values of $\tilde{l}_D$ are shown as red squres in Figs. 6. The blue lines are error bars, and data with dark bars indicate that the error is so big or the convergence of fitting is so poor that the data are not reliable. They show that the measured diffusion length becomes a steady value consistent with the diffusion length expected from the source velocity: $\tilde{l}_D \approx l_D \equiv D_s/V_p$. Because of the large error, the initial behavior is not very clear, but Fig. 6(c) indicates that $\tilde{l}_D$ is small in the initial stage and increases up to the steady value. This is reasonable since the source is initially close to the step.

Interpretatin of the change in period. Interpretation of the results is not simple. The first stages in the Fourier analysis (Fig. 4) and in the branch number analysis (Fig. 3) show similar exponents: about 1/4 with $V_p = 0.02$ slightly increasing

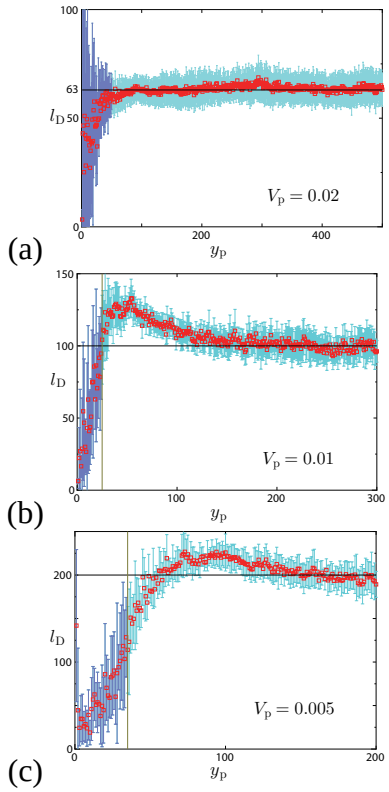

Figure 6: Change of the measured diffusion length $\tilde{l}_D$ as time (red squares with a blue error bar) with the source velocity (a) $V_p = 0.02$. (b) $V_p = 0.01$. (c) $V_p = 0.005$. The data with a dark error bar indicate fitting is poor and unreliable.

with decreasing V_p. Crossover to the second stage is seen in both analyses, but the change from the first stage in Fig. 4 occurs about three times later than in Fig. 3. We think the change in the first stage is due to local relaxation of a rough step formed by random attachment of adatoms although we do not have theoretical explanation of the exponent. The snapshot of the step in Fig. 7(a) shows a pattern in this stage. This process continues as observed in the Fourier analysis, and wandering instability occurs in addition. In Fig. 7(c) the instability is obvious and not all intrusions are detected by the branch counting. The intrusions formed by the instability begin to compete. Such a feature becomes evident in Fig. 7(d) when only winners of the competition are counted. Fig. 7(b) is a snapshot at the crossover point in Fig. 3(b). The first stage observed in Fig. 4 ends when λ becomes about λ_{max} of Eq. (3). Implication of this result and its relation to the change in the diffusion length are still unsolved problem to us.

In the second stage, the exponent is about 1/2. Observation of many growth patterns suggests that the coarsening proceeds by competition of intrusions as seen in Figs. 7(c) and (d). If we start with intrusions of a comparable size with period λ_1, the natural selection of winners takes time $t \sim \lambda_1^2$ since it is the result of disparity in the diffusion field. This may be the origin of the exponent close to 1/2, as often seen in step growth phenomena [13, 14].

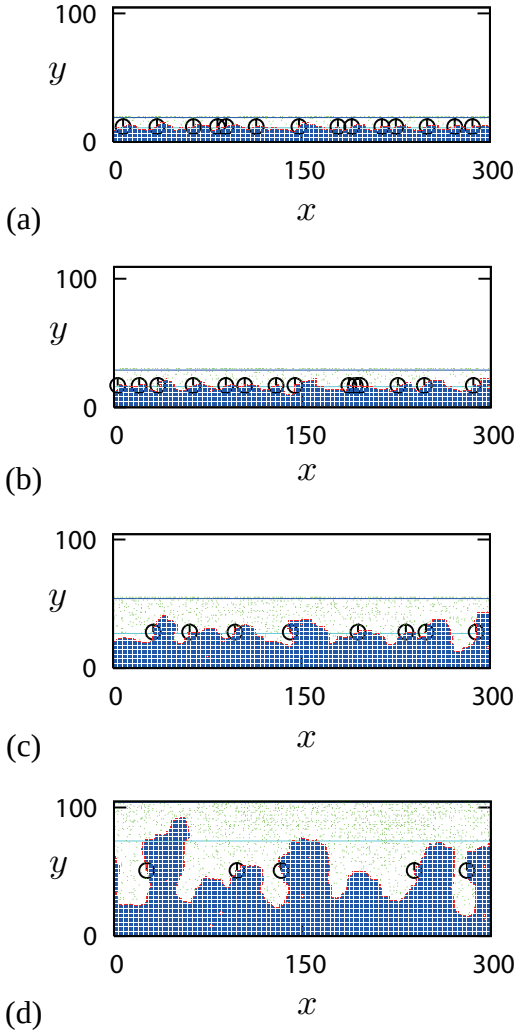

Figure 7: Step patterns with $V_p = 0.01$ at (a) $t = 1500$, (b) $t = 2500$, (c) $t = 5000$, (b) $t = 10000$. Circles indicate the position of branches couted in Fig. 3.

5. Response to an abrupt change in the velocity

Since the period of the branches in the steady state, λ^*, is determined by the velocity of the source V_p, it must respond to an abrupt change in the velocity. In the case of thin-film lamellar eutectic growth, doubling of the pulling rate induces a parity breaking transition and a tilted pattern is seen [15]. To find out the way branches adjust their shape to a new period that corresponds to the new source velocity, we performed simulations in which V_p jumps to a value several times larger or smaller than the initial one when the source reaches $y_p = 700$.

Increase of the source velocity. Severel examples for the growth into the [11] direction, toward which branches tend to grow straight with less branching, are shown in Figs. 8 and 9. Fig. 8(a) and (b) are step patterns when the velocity has increased nine times. With our standard value of the stiffness $\epsilon/k_BT = 2.0$, after the initial coarsening, the number of survived branches in the view (a) is three. The favorable number of branches for the nine times increase of V_p is $3 \times \sqrt{9} = 9$. In (a), two

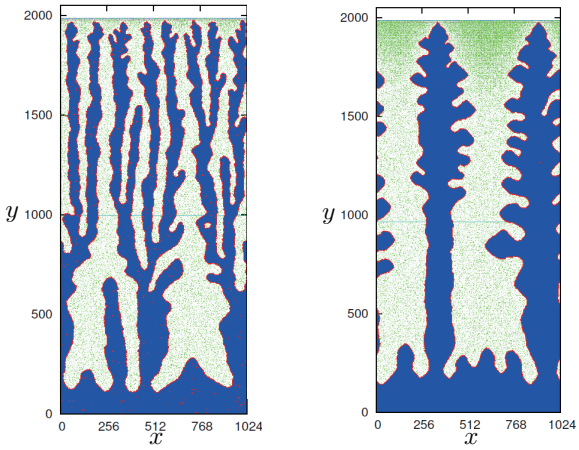

Figure 8: Step patterns with the change from $V_p = 0.000866$ to 0.007793 (9 times increase). (a) $\epsilon/k_BT = 2.0$, (b) $\epsilon/k_BT = 3.0$.

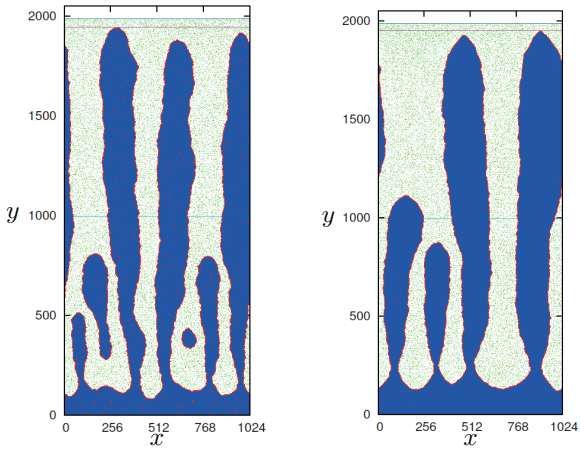

Figure 9: Step patterns with the change from $V_p = 0.007793$ to 0.000866 (9^{-1} times). (a) $\epsilon/k_BT = 2.0$, (b) $\epsilon/k_BT = 3.0$.

branches out of the three made multiple tip-splitting and the number of branches takes values from seven to nine depending on the height. With larger stiffness $\epsilon/k_BT = 3.0$, the number in the first steady state is two as seen in (b). After the change in V_p, the favorable number would be six, but the number remained the same. Because of the large stiffness, tip-splitting hardly occurs and instead side-branching occurs to compensate the large separation between the main branches. Transition to a state of different number of branches is a discontinuous transition and a large fluctuation is necessary, as in a first order phase transition. It is only possible with weak anisotropy of the stiffness.

Decrease of the source velocity. When the source velocity V_p is decreased, the favorable number of branches decreases. Contrary to the case of increasing velocity, termination of growth of some existing branches is sufficient to realize a state with fewer branches. Figs. 9(a) and (b) show patterns formed by a sudden decrease of V_p by 1/9. With $\epsilon/k_BT = 2.0$, the number decreased from seven to three (several branches in Fig. 9(a) are already broken and about to dissapear by local relaxation), and from four to two with $\epsilon/k_BT = 3.0$. Note that the most favorable number of branches is expected to appear only on average, and that the actual number is also limited by the system size.

6. Summary and discussion

We have examined coarsening process of the branch period in the step wandering instability guided by a linear source of adatoms. Our model was motivated by the step pattern on a Ga deposited Si(111) surface, and is possibly applicable to the finger pattern of a graphene sheet grown from SiC. In the first stage the period increases as $\lambda \sim t^{\nu_1}$, with $\nu_1 \approx 1/4$, increasing slowly with decreasing V_p. In the Fourier analysis, this behavior continues untill $\lambda \sim \lambda_{max}$, where λ_{max} is the most unstable wavelength for the diffusion length in the steady state. However, the competition between the intrusions results in a faster growth of the branch period with the exponent $\nu_2 \approx 1/2$. With an abrupt change in the velocity, branches adjust their period by terminating growth of some branches or by increasing their number by tip-splitting. The latter is suppressed by a large stiffness, and a metastable state with side branches is seen.

Theoretically, many questions arise. The branch period, λ^*, in the steady state is apparently related to the wavelength λ_{max} of the most unstable mode, but it is several times larger than λ_{max}. How is the prefactor determined? Can one explain the coarsening exponents $\nu_1 \approx 1/4$ and $\nu_2 \approx 1/2$? Are they related to the change in diffusion length? Certainly crystal anisotropy is essential to the step pattern as observed in the metastable state under the abrupt change in the source velocity. Quantitative study of the effect of anisotropy is necessary if one wishes to control the shape.

The present study was supported by Grants-in-Aid from Japan Society for the Promotion of Science.

References

[1] H. Hibino, H. Kageshima, and M. Uwaha, Surf. Sci. **602** (2008) 2421.
[2] M. Sato, S. Kondo, and M. Uwaha, J. Cryst. Growth, **318** (2011) 14.
[3] S. Kondo, M. Sato, M. Uwaha, and H. Hibino, Phys. Rev. B, to be published.
[4] V. Borovikov and A. Zangwill, Phys. Rev. B **80** (2009) 121406(R).
[5] M. L. Bolen, S. E. Harrison, L. B. Biedermann, and M. A. Capano, Phys. Rev. B **80** (2009) 115433.
[6] T. Ohta, N. C. Bartelt, S. Nie, K. Thürmer, and G. L. Kellogg, Phys. Rev. B **81** (2010) 121411(R).
[7] I. Bena, C. Misbah, and A. Valance, Phys. Rev. B**47** (1993) 7408.
[8] M.Uwaha and Y.Saito, Phys. Rev. Lett. **68** (1992) 224; Y. Saito and M. Uwaha, Phys. Rev. B **49** (1994) 10677.
[9] T. Maroutian, L. Douillard and H.-J. Ernst, Phys. Rev. B **64** (2001) 165401.
[10] O. Pierre-Louis, C. Misbah, Y. Saito, J. Krug, and P. Politi, Phys. Rev. Lett. **80** (1998) 4221.
[11] F. Gillet, O. Pierre-Louis and C. Misbah, Eur. Phys. J. B **18** (2000) 519.
[12] S. Paulin, F. Gillet, O. Pierre-Louis, and C. Misbah, Phys. Rev. Lett. **86** (2001) 5538.
[13] M. Sato and M. Uwaha, J. Phys. Soc. Jpn. **67** (1998) 3675.
[14] M. Sato and M. Uwaha, Surf. Sci. **493** (2001) 494.
[15] G. Faivre and J. Mergy, Phys. Rev. A **46** (1992) 963.